

Ultra-wide bandgap amorphous oxide semiconductors for NBIS-free thin-film transistors

Cite as: *APL Mater.* **7**, 022501 (2019); <https://doi.org/10.1063/1.5053762>

Submitted: 25 August 2018 • Accepted: 02 October 2018 • Published Online: 07 December 2018

 Junghwan Kim, Joonho Bang, Nobuhiro Nakamura, et al.

COLLECTIONS

Paper published as part of the special topic on [Wide Bandgap Oxides](#)



View Online



Export Citation



CrossMark

ARTICLES YOU MAY BE INTERESTED IN

[Hydrogen anion and subgap states in amorphous In-Ga-Zn-O thin films for TFT applications](#)

Applied Physics Letters **110**, 232105 (2017); <https://doi.org/10.1063/1.4985627>

[Control of O-H bonds at a-IGZO/SiO₂ interface by long time thermal annealing for highly stable oxide TFT](#)

AIP Advances **7**, 125110 (2017); <https://doi.org/10.1063/1.5008435>

[Effects of excess oxygen on operation characteristics of amorphous In-Ga-Zn-O thin-film transistors](#)

Applied Physics Letters **99**, 093507 (2011); <https://doi.org/10.1063/1.3633100>

AMERICAN ELEMENTS
THE ADVANCED MATERIALS MANUFACTURER®

ultra-high purity materials
epitaxial crystal growth
carbon nanotubes
rare earth metals
silicon nanoparticles
MO/CVD
rare earth metals
diamond
refractory metals
oxide
chalcogenides
perovskite crystals

ultra-high purity materials
epitaxial crystal growth
carbon nanotubes
rare earth metals
silicon nanoparticles
MO/CVD
rare earth metals
diamond
refractory metals
oxide
chalcogenides
perovskite crystals

ultra-high purity materials
epitaxial crystal growth
carbon nanotubes
rare earth metals
silicon nanoparticles
MO/CVD
rare earth metals
diamond
refractory metals
oxide
chalcogenides
perovskite crystals

ultra-high purity materials
epitaxial crystal growth
carbon nanotubes
rare earth metals
silicon nanoparticles
MO/CVD
rare earth metals
diamond
refractory metals
oxide
chalcogenides
perovskite crystals

ultra-high purity materials
epitaxial crystal growth
carbon nanotubes
rare earth metals
silicon nanoparticles
MO/CVD
rare earth metals
diamond
refractory metals
oxide
chalcogenides
perovskite crystals

ultra-high purity materials
epitaxial crystal growth
carbon nanotubes
rare earth metals
silicon nanoparticles
MO/CVD
rare earth metals
diamond
refractory metals
oxide
chalcogenides
perovskite crystals

ultra-high purity materials
epitaxial crystal growth
carbon nanotubes
rare earth metals
silicon nanoparticles
MO/CVD
rare earth metals
diamond
refractory metals
oxide
chalcogenides
perovskite crystals

ultra-high purity materials
epitaxial crystal growth
carbon nanotubes
rare earth metals
silicon nanoparticles
MO/CVD
rare earth metals
diamond
refractory metals
oxide
chalcogenides
perovskite crystals

ultra-high purity materials
epitaxial crystal growth
carbon nanotubes
rare earth metals
silicon nanoparticles
MO/CVD
rare earth metals
diamond
refractory metals
oxide
chalcogenides
perovskite crystals

Now Invent.™

www.americanelements.com

The Next Generation of Material Science Catalogs

Ultra-wide bandgap amorphous oxide semiconductors for NBIS-free thin-film transistors

Cite as: APL Mater. 7, 022501 (2019); doi: 10.1063/1.5053762

Submitted: 25 August 2018 • Accepted: 2 October 2018 •

Published Online: 7 December 2018



View Online



Export Citation



CrossMark

Junghwan Kim,^{1,a)}  Joonho Bang,¹ Nobuhiro Nakamura,^{1,2} and Hideo Hosono^{1,3,a)}

AFFILIATIONS

¹Materials Research Center for Element Strategy, Tokyo Institute of Technology, Mailbox SE-6, 4259 Nagatsuta, Midori-ku, Yokohama 226-8503, Japan

²New Product R&D Center, Asahi Glass Co. Ltd., 1150, Hazawa, Kanagawa-ku, Yokohama 221-8755, Japan

³Laboratory for Materials and Structures, Institute of Innovative Research, Tokyo Institute of Technology, Mailbox R3-4, 4259 Nagatsuta, Midori-ku, Yokohama 226-8503, Japan

^{a)}Authors to whom correspondence should be addressed: JH.KIM@mces.titech.ac.jp and hosono@msl.titech.ac.jp

ABSTRACT

The transparency of oxide semiconductors is a significant feature that enables the fabrication of fully transparent electronics. Unfortunately, practical transparent electronics using amorphous oxide semiconductors (AOSs) have not yet been realized, owing to significant photo-instabilities of these materials. Previous studies have revealed that the photo-instability can be attributed to sub-gap states (SGSs) near the valence-band maximum (VBM). Thus, it is inferred that the energy difference between the SGSs and the conduction-band minimum must be widened sufficiently in order to make it fully transparent over the entire visible-light region. In this work, we examined the electronic structures of a variety of AOSs and found that their ionization potentials vary greatly, depending upon the specific metal cations. This finding enabled us to increase the optical bandgap by modifying the VBM levels, resulting in a high mobility of 9 cm²/Vs and an ultra-wide bandgap of 3.8 eV for amorphous Zn-Ga-O (a-ZGO). We show that a-ZGO thin-film transistors exhibit no negative-bias illumination-stress instability with no passivation and no light-shielding layer.

© 2018 Author(s). All article content, except where otherwise noted, is licensed under a Creative Commons Attribution (CC BY) license (<http://creativecommons.org/licenses/by/4.0/>). <https://doi.org/10.1063/1.5053762>

The first thin-film transistor (TFT) with an amorphous oxide semiconductor (AOS) as the channel layer was demonstrated in 2004.¹ Since then, AOSs have attracted considerable attention, owing to their outstanding properties, such as high electron mobility, low-temperature processability, good uniformity, and high transparency.¹ As a result, AOS-TFTs are now employed as backplanes to drive pixels in state-of-the-art flat-panel displays (FPDs).

However, a critical technical issue remains to be solved for better device applications. Although AOSs are highly transparent in the visible range, many studies have reported that they have photo-instabilities, such as negative-bias illumination stress (NBIS). In particular, the NBIS issue hampers the realization of fully transparent AOS electronics; a light-shielding layer is currently used as a temporary expedient. It has been reported that AOSs exhibit photo-sensitivity to

light with smaller photon energies than their bandgaps (E_g).^{2,3} A hard X-ray photoemission study (HAX-PES), which can be applied to as-prepared thin films and which has a large ionization cross section for s-state electrons, revealed the existence of high-density defect states (10^{19} – 10^{20} cm⁻³) near the valence-band maximum (VBM)—hereafter termed “sub-gap states,” (SGSs)⁴—in AOS thin films, as shown in Fig. 1(a). The photo-sensitivity to sub-gap light (below ~2.3 eV) is attributed to the excitation of electrons from the SGSs to the conduction-band minimum (CBM). Several models for these defects have been proposed, such as oxygen vacancies, weakly bonded oxygen, and hydrogen impurities.^{5,6}

With this background, we conclude that there are two possible approaches to resolving the photo-instability issue of AOS-TFTs: (i) elimination of the SGSs [Fig. 1(b)] or (ii) widening the optical bandgap to keep the photoexcitation

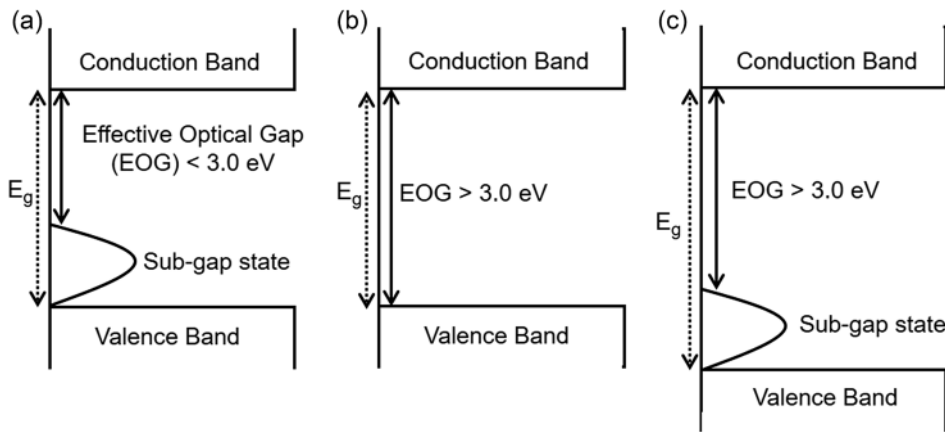


FIG. 1. Schematic energy structure of (a) a conventional AOS and two possible approaches to photo-stable AOSs, (b) elimination of the sub-gap states (SGSs) above the valence-band maximum (VBM), and (c) widening the optical bandgap to keep the excitation energy between the SGSs and the conduction-band minimum (CBM) $> 3.0 \text{ eV}$.

energy between the SGSs and the CBM larger than $\sim 3 \text{ eV}$ [Fig. 1(c)].

To confirm the effect of the SGSs on NBIS, we compared two amorphous InGaZnO_x (a-IGZO) TFTs with low and high SGSs, respectively, as shown in Fig. 2(a). We reduced the SGSs by using ultra-high vacuum sputtering (base pressure: $\sim 3 \times 10^{-7} \text{ Pa}$), and we prepared IGZO films with high SGSs using pulsed laser deposition (base pressure: $\sim 3 \times 10^{-5} \text{ Pa}$). The difference in the SGSs may be caused by the reduction in the residual hydrogen in the chamber.^{7,8} We fabricated bottom-gate TFTs using 40 nm thick a-IGZO (In:Ga:Zn = 1:1:1) films on $\text{SiO}_2/\text{p}^+\text{-Si}$ substrates.⁹ The channel width and length were 300 and 50 μm , respectively. We conducted post-annealing of the films at 400 $^\circ\text{C}$ in an O_2 atmosphere. We performed the NBIS tests with a gate voltage of -20 V for a stress duration of 3600 s at room temperature. We illuminated these a-IGZO TFTs using a white light-emitting diode (LED) of 11 000 lux. The results shown in Figs. 2(a)–2(c) definitely confirm that the SGSs are responsible for the NBIS instability; the IGZO TFT with higher SGSs exhibited a larger shift in threshold voltage (V_{th}), $\sim 11 \text{ V}$, whereas the IGZO TFT with the low SGSs exhibited a V_{th} shift of $\sim 7 \text{ V}$. However, this V_{th} shift is still insufficient for the TFTs used to drive FPDs without compensation. The elimination of SGSs by removing the hydrogen impurities and/or oxygen vacancies to a negligible level seems not

to be a practical solution because the AOS TFTs fabricated by conventional mass-production processes contain hydrogen impurities comparable with the SGSs.^{10,11}

Consequently, widening the E_g will be a more practical approach if the location of the SGSs is pushed down with the VBM. The E_g of an AOS can be widened readily by tuning its chemical composition. However, widening the E_g alone does not guarantee the electrical properties; a wide E_g with high mobility is the criterion for practical use. The high electron mobility of the AOSs is understood from their electronic structural nature. For AOSs, the CBM is composed of metal-cation-vacant s-orbitals, whereas the VBM is formed by oxygen 2p-orbitals.¹² The spatial overlap between the vacant s-orbitals of p-block metal cations is insensitive to structural randomness, which explains why the high mobility of AOSs is retained even in amorphous structures. This is the major reason why conventional AOSs consisting of heavier post-transition-metal cations exhibit higher mobility via the small effective mass of the electrons.¹³ However, large dispersion of the conduction band, in general, leads to a deep conduction-band-minimum level (E_{CBM}) and a narrow E_g , as illustrated in Fig. 3(b). On the contrary, AOSs that include light-metal cations such as Al and Si exhibit a wider E_g , but the higher E_{CBM} makes it impossible to dope the electrons,¹⁴ and the small band dispersion leads to small mobility¹⁵ [see Fig. 3(c)].

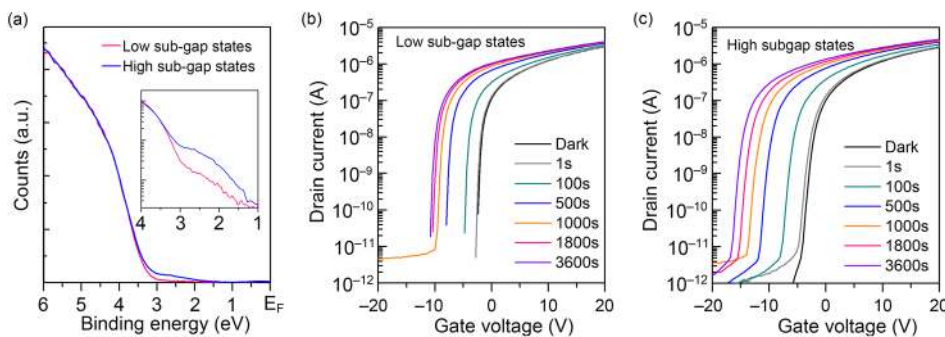


FIG. 2. (a) HAX-PES results for amorphous InGaZnO_x (a-IGZO) thin films with high and low sub-gap states (SGSs). Results of the NBIS test of a-IGZO TFTs with low SGSs (b) and high SGSs (c). The conditions of the NBIS tests are described in the text.

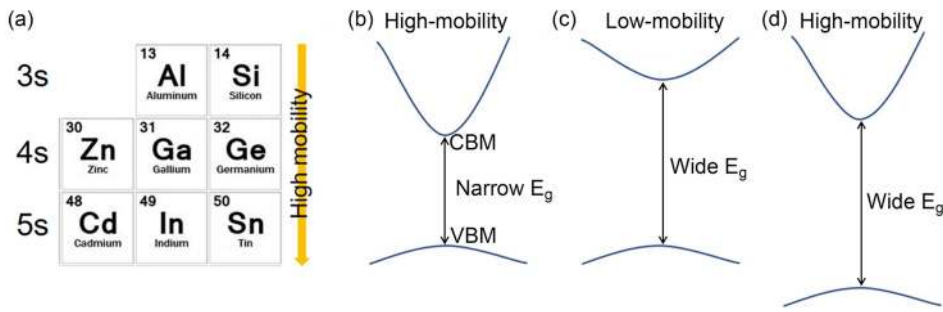


FIG. 3. Possible cation candidates for AOSs with large electron mobilities (a). The expected electronic structures and electrical properties of conventional AOSs with (b) high electron mobility and a narrow E_g , (c) low electron mobility and a wide E_g , and (d) a proposed electronic structure with suitable photo-stability and high mobility.

We thus infer that a wide E_g with high mobility will be attained if we can deepen just the valence-band-maximum level (E_{VBM}) while retaining a large conduction-band dispersion [see Fig. 3(d)].

We recently found that amorphous Zn-Ga-O (a-ZGO) exhibits a large variation in E_{VBM} , corresponding to ionization potential (I.P.), whereas E_{CBM} remains almost unchanged.^{16,17} The I.P. alteration is attributable to a contribution of Zn 3d-orbitals to the formation of covalent bonding with the O 2p-orbitals; the Zn 3d-O 2p interaction makes the E_{VBM} corresponding to the anti-bonding level shallow.¹⁸ On the other hand, a-GaO_x has a very deep I.P. of 8.2 eV. Consequently, a-ZGO exhibits a large variation of E_{VBM} , depending upon the Zn/Ga ratio. We investigated a-ZGO thin films and compared the energy levels of amorphous In-Zn-O (IZO) and a-ZGO using *in situ* ultra-violet photoemission spectroscopy (UPS).

The values of E_{CBM} , E_{VBM} , and E_g are summarized in Table S1. The UPS results in Fig. 4(a) indicate that the AOSs tend to have deeper E_{CBM} with increased In content, as expected. On the other hand, the contribution of Zn 3d to E_{VBM} was clearly observed, as shown in Fig. 4(b). Further, the deeper E_{VBM} of a-ZGO than a-IZO seems attributable to the intrinsic nature GaO_x, which has a very deep I.P. (8.2 eV). Thus, we conclude that (i) In/Zn should be avoided and (ii) GaO_x with a deep I.P. should be included as much as possible. As shown in Fig. 4 and Table S1, we note that the a-IZO system is inappropriate for the present purpose, due to its narrow E_g .

Finally, we confirmed that a TFT of a-Zn_{0.3}Ga_{0.7}O_x (a-ZGO) has excellent photo-stability. Figure 5 shows the results of the NBIS instability tests on a-ZGO TFTs, together with a-IZO and a-IGZO TFTs. The a-IZO TFT exhibited the worst photo-stability,¹⁹ a V_{th} shift of ~11 V and degradation

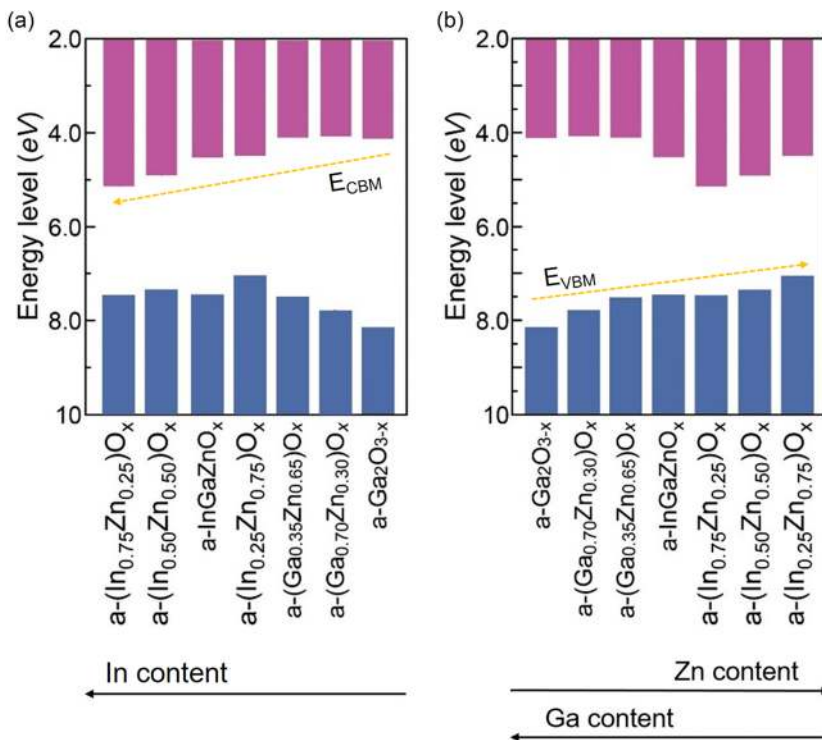


FIG. 4. Energy levels of various AOSs determined by *in situ* UPS, which are arranged in order of (a) conduction band minimum (CBM) level and (b) valence band maximum (VBM) level, respectively.

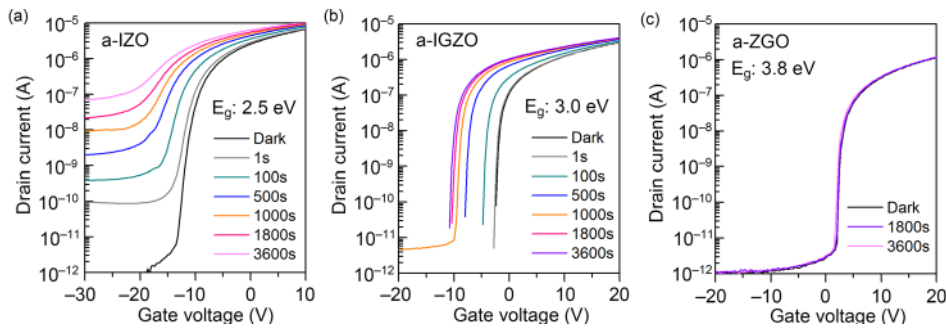


FIG. 5. NBIS test results for TFTs fabricated from (a) $\text{In}_{0.5}\text{Zn}_{0.5}\text{O}_x$ ($E_g = 2.5$ eV), (b) InGaZnO_x ($E_g = 3.0$ eV), and (c) $\text{Zn}_{0.3}\text{Ga}_{0.7}\text{O}_x$ ($E_g = 3.8$ eV).

of the on/off ratio. The degradation of the on/off ratio may be attributed to a band-to-band excitation by the white LED because the maximum photon energy of the white LED is $h\nu \sim 2.8$ eV, which is larger than the E_g of a-IZO. On the other hand, the a-ZGO TFT exhibited excellent photo-stability, with almost no observed V_{th} shift. This result implies that the energy difference between the SGSs and the CBM of a-ZGO is larger than ~ 3.0 eV. The saturation mobility of the a-ZGO TFT was ~ 9 cm^2/Vs , whereas those of the a-IZO and a-IGZO TFTs were ~ 40 and ~ 15 cm^2/Vs , respectively. The mobility of 9 cm^2/Vs is the lowest among these three systems, but it is an order of magnitude larger than that of an a-Si:H TFT, and it satisfies the current specifications for backplanes to drive FPDs; it is thus expected that a-ZGO as UWB-AOSs will be an appropriate material for fully transparent electronics.

In conclusion, we reported that widening the band gap is an effective approach to suppressing the photosensitivity of AOSs. In particular, lowering the E_{VBM} is critical to suppressing NBIS instability. We found that excellent NBIS stability, while retaining a mobility of ~ 9 cm^2/Vs , was attained in a-ZGO system with a deep E_{VBM} of ~ 7.8 eV and an ultra-wide bandgap of ~ 3.8 eV. The mobility and photo-stability are generally in conflict; the mobility increases with the In content, but photo-stability is degraded. The a-ZGO system appears to offer a good compromise between mobility and photo-stability, making it a good candidate semiconductor for fully transparent TFTs.

See [supplementary material](#) for the electron affinity (E_{CBM}), ionization potential (E_{VBM}), and bandgap (E_g) values of relevant AOSs.

We thank Dr. S. Ueda at the National Institute for Materials Science (NIMS) for the assistance of HAXPES measurement. This work was supported by the Ministry of Education, Culture, Sports, Science and Technology (MEXT) through Element

Strategy Initiative to Form Core Research Center. J. Kim was also supported by the JSPS through a Grant-in-Aid for Young Scientists (Grant No. 17K14548).

REFERENCES

- 1 K. Nomura, H. Ohta, A. Takagi, T. Kamiya, M. Hirano, and H. Hosono, *Nature* **432**, 488 (2004).
- 2 H. Jung, Y. Kang, A. Hwang, C. Lee, S. Han, D. Kim, J. Bae, W. Shin, and J. Jeong, *Sci. Rep.* **4**, 3765 (2014).
- 3 K. Lee, J. Jung, K. Son, J. Park, T. Kim, R. Choi, J. Jeong, J. Kwon, B. Koo, and S. Lee, *Appl. Phys. Lett.* **95**, 232106 (2009).
- 4 K. Nomura, T. Kamiya, H. Yanagi, E. Ikenaga, K. Yang, K. Kobayashi, M. Hirano, and H. Hosono, *Appl. Phys. Lett.* **92**, 202117 (2008).
- 5 K. Ide, Y. Kikuchi, K. Nomura, M. Kimura, T. Kamiya, and H. Hosono, *Appl. Phys. Lett.* **99**, 093507 (2011).
- 6 K. Ji, J. Kim, H. Jung, S. Park, R. Choi, U. Kim, C. Hwang, D. Lee, H. Hwang, and J. Jeong, *Appl. Phys. Lett.* **98**, 103509 (2011).
- 7 J. Bang, S. Matsuishi, and H. Hosono, *Appl. Phys. Lett.* **110**, 232105 (2017).
- 8 T. Miyase, K. Watanabe, I. Sakaguchi, N. Ohashi, K. Domen, K. Nomura, H. Hiramatsu, H. Kumomi, H. Hosono, and T. Kamiya, *ECS J. Solid State Sci. Technol.* **3**, Q3085 (2014).
- 9 J. Kim, N. Nakamura, T. Kamiya, and H. Hosono, *SID Int. Symp. Dig. Tech. Pap.* **47**, 951 (2016).
- 10 Y. Nam, H. Kim, S. Cho, and S. Park, *RSC Adv.* **8**, 5622 (2018).
- 11 A. Tari and W. Wong, *Appl. Phys. Lett.* **112**, 073506 (2018).
- 12 T. Jun, J. Kim, M. Sasase, and H. Hosono, *Adv. Mater.* **30**, 1706573 (2018).
- 13 H. Hosono, *J. Non-Cryst. Solids* **352**, 851 (2006).
- 14 H. Hosono, *Jpn. J. Appl. Phys., Part 1* **52**, 090001 (2013).
- 15 N. Nakamura, J. Kim, and H. Hosono, *Adv. Electron. Mater.* **4**, 1700352 (2018).
- 16 J. Kim, T. Sekiya, N. Miyokawa, N. Watanabe, K. Kimoto, K. Ide, Y. Toda, S. Ueda, N. Ohashi, H. Hiramatsu, H. Hosono, and T. Kamiya, *NPG Asia Mater.* **9**, e359 (2017).
- 17 J. Kim, N. Miyokawa, T. Sekiya, K. Ide, Y. Toda, H. Hiramatsu, H. Hosono, and T. Kamiya, *Thin Solid Films* **614**, 84 (2016).
- 18 T. Kamiya and M. Kawasaki, *MRS Bull.* **33**, 1061 (2008).
- 19 S. Park, J. Song, C. Lee, B. Son, C. Lee, H. Kim, R. Choi, Y. Choi, U. Kim, C. Hwang, H. Kim, and J. Jeong, *IEEE Electron Device Lett.* **34**, 894 (2013).